

Synthesis, DNA-binding, Cytotoxicity, Photo Cleavage, Antimicrobial and Docking Studies of Ru(II) Polypyridyl Complexes

A. Srishailam · Yata Praveen Kumar · Nazar M. D. Gabra ·
P. Venkat Reddy · N. Deepika · Nageeti Veerababu ·
S. Satyanarayana

Received: 6 February 2013 / Accepted: 24 February 2013 / Published online: 4 April 2013
© Springer Science+Business Media New York 2013

Abstract Three Ruthenium(II) polypyridine complexes, $[\text{Ru}(\text{phen})_2(\text{mipc})]^{2+}$ (1), $[\text{Ru}(\text{bpy})_2(\text{mipc})]^{2+}$ (2) and $[\text{Ru}(\text{dmb})_2(\text{mipc})]^{2+}$ (3) [mipc=2-(6-methyl-3-(1H-imidazo[4, 5-f][1,10]-phenanthroline-2-yl)-4H-chromene-4-one, phen=1,10-phenanthroline, bpy=2, 2'bipyridine, dmb=4, 4'-dimethyl-2, 2'-bipyridine] have been synthesized and characterized by elemental analysis, IR, UV–Vis, ^1H & ^{13}C NMR and mass spectra. The DNA-binding properties of the Ruthenium(II) complexes were investigated by spectrophotometric methods, viscosity measurements and light switch studies. These three complexes have been focused on photo activated cleavage studies with pBR-322 and antimicrobial studies. Experimental results indicate that the three complexes intercalate into DNA base pairs and follows the order of $1 > 2 > 3$ respectively. Molecular docking studies also support the DNA interactions with complexes through hydrogen bonding and vander Waal's interactions. Cytotoxicity studies with Hela cell lines has been revealing about anti tumor activity of these complexes.

Keywords Cytotoxicity · Anti tumor activity · Antimicrobial · Intercalation and docking

A. Srishailam · Y. P. Kumar · N. M. D. Gabra · P. V. Reddy ·
N. Deepika · S. Satyanarayana (✉)
Department of Chemistry, Osmania University,
Hyderabad, India 500007
e-mail: ssnirasani@gmail.com

N. Veerababu
Department of Biochemistry, Osmania University,
Hyderabad, India 500007

Introduction

For half a century, the field of metal-based anticancer drugs has been dominated by the precious metal platinum [1, 2]. It is not effective in many common types of cancers, drug resistance is common and it has a deplorable range of side effects, which can include nerve damage, hair loss and nausea. Enthusiastic researchers all over the world are concentrating on synthesizing new metal complexes to overcome these limitations (Sn, Ni, Cu, Au, Pd and Ru) [3–5]. Passionate work about some ruthenium complexes have been developed and tested against cancer cell lines, known for their antitumor activity against mouse leukemia L1210 cells, human oral epidermoid carcinoma KB cells, human promyelocytic leukemia cells (HL-60) and liver cancer cells [6–9]. Also these complexes have been utilized in the design and development of synthetic restriction enzymes, chemotherapeutic drugs, DNA foot printing agents and stereo selective probes of nucleic acid structure [10–19]. Drugs based on ruthenium such as NAMI-A, KP1019 and $(\text{ImH}[\text{transRu}(\text{III})\text{Cl}_4\text{Im}(\text{DMSO})])$ [20, 21], are under clinical trials for metastatic and colorectal cancers. Ru(II) polypyridyl complexes have the possibility of becoming anticancer agents, because they are effective against primary tumors. Recently, Sadler and his co-workers have reported half-sandwich Ru(II) arene complexes, which exhibit reproducible anticancer activity against A2780 human ovarian cancer cell lines both in vitro and in vivo [22]. Since DNA has been identified as the possible primary molecular target of metal-based anticancer agents such as cisplatin, attention is mainly focused on interacting ruthenium complexes with DNA to identify whether DNA binding is effective and whether they can act as chemotherapeutic agents.

The introduction of the substituted chromene in 2-(6-methyl-3-(1H-imidazo [4, 5-f][1, 10]-phenanthroline-2-yl)-4H-chromene-4-one (mipc) may provide an opportunity to search the photoprobes of DNA and therapeutic reagents. Carbonyl oxygen of chromene and imidazo ring of mipc group forms hydrogen bonds and van der Waal's interactions with backbone (phosphate oxygens), sugar and bases of DNA molecule. This was observed by docking studies with computational work by using GOLD DOCK software.

As Sauvage et al. and Barton groups observed [23, 24], the MLCT luminescence as light-induced charge transfers directed from ruthenium atom to π^* orbital of mipc ligand ($d_{Ru} \rightarrow \pi^*_{mipc}$). Our complexes bind to DNA with intense MLCT luminescence on the addition of DNA, whereas luminescence of the unbound complex is quenched. This phenomenon, which has become known as the DNA "light switch" effect, has been exclusively used to study the interaction of metal polypyridyl complexes with DNA through intersystem crossing from 1MLCT to 3MLCT by using fluorescence spectroscopy [25]. Recently, good progressive work has been done by our group on Ru(II) polypyridyl complexes [26–35]. In this article we are focusing on Ru(II) polypyridyl complexes 1, 2 and 3, their antitumor cell activities were evaluated by MTT (3-(4, 5-dimethylthiazol-2-yl)-2, 5-diphenyltetrazolium bromide) assay with Hela cancer cell lines. Viscosity, thermal denaturation studies, abilities to induce cleavage of pBR-322 DNA, and antimicrobial studies have given supporting data for these complexes. Binding of ruthenium complexes remains an issue of rigorous debate with factors such as size, shape and planarity of the intercalative ligand, and changing substituent group or substituted position on the intercalative ligand influencing the DNA-binding mechanism [35–39].

Experimental

Materials

$RuCl_3$, 1, 10-Phenanthroline, 2, 2'-bipyridine, 4, 4'-dimethyl-2, 2'-bipyridine and 2-(6-methyl-3-Chromyl) were purchased from Sigma. The super coiled (CsCl purified) pBR-322 DNA (Bangalore, Genie, India) was used as received. All other chemicals and solvents were procured from local available sources. All the solvents were purified before use as per standard procedures [40]. The Spectroscopic titration was carried out in the buffer (5 mM Tris-HCl, 50 mM NaCl, pH 7.2) at room temperature. Solutions of DNA in Tris-HCl buffer (pH=7.2), 50 mM NaCl gave a ratio of UV absorbance at 260 and 280 nm of 1.8–1.9, indicating that the DNA was sufficiently free of protein [41]. The concentration of CT-DNA was determined spectrophotometrically using the molar absorption $6,600 M^{-1} cm^{-1}$ (260 nm)[42]. For docking studies GOLD, Mercury software was used. Cis-Platin and MTT

(3-(4, 5-dimethylthiazol-2-yl)-2, 5-diphenyltetrazolium bromide) were purchased from Sigma.

Methods

Compounds 1, 10-phenanthroline-5, 6-dione, cis-[Ru(phen)₂Cl₂]. 2H₂O, cis-[Ru(bpy)₂Cl₂]. 2H₂O, cis-[Ru(dmb)₂Cl₂]. 2H₂O [43, 44] were prepared according to methods in literature.

Synthesis of [Ru(phen)₂(mipc)](ClO₄)₂. 2H₂O

Cis-[Ru(phen)₂Cl₂]. 2H₂O and mipc was dissolved in a mixture of ethanol (25 ml) and water (15 ml), reflux it with 120°C for 8 h under N₂- atmosphere to give a clear red solution. Upon cooling the solution was treated with saturated aq. solution of NaClO₄ to give brick red ppt. Then it washed with CH₃CN-Toluene (3:1) and vacuum dried. Yield 0.364 g (68.48 %). C₄₇H₃₄Cl₂N₈O₁₂Ru (Anal. Calc. for C₄₇H₃₄Cl₂N₈O₁₂Ru: C, 52.52; H, 3.19; N, 10.43. Found: C, 52.49; H, 3.15; N, 10.46 %). ESMS [CH₃CN, m/z]: 939.

Synthesis of [Ru(bpy)₂(mipc)](ClO₄)₂. 2H₂O

This Complex was synthesized with similar procedure of the above complex (1), with cis-[Ru(phen)₂Cl₂].2H₂O (0.2620 g, 0.5 mmol) in place of cis-[Ru(bpy)₂Cl₂].2H₂O. Yield: 0.370 g (73.34 %). (Anal. Calc. for C₄₇H₃₄Cl₂N₈O₁₂Ru: C, 50.30; H, 3.34; N, 10.91. Found: 0.370 g, 74.81 %. C, 50.34; H, 3.32; N, 10.94 %). ESMS [CH₃CN, m/z]: 891.

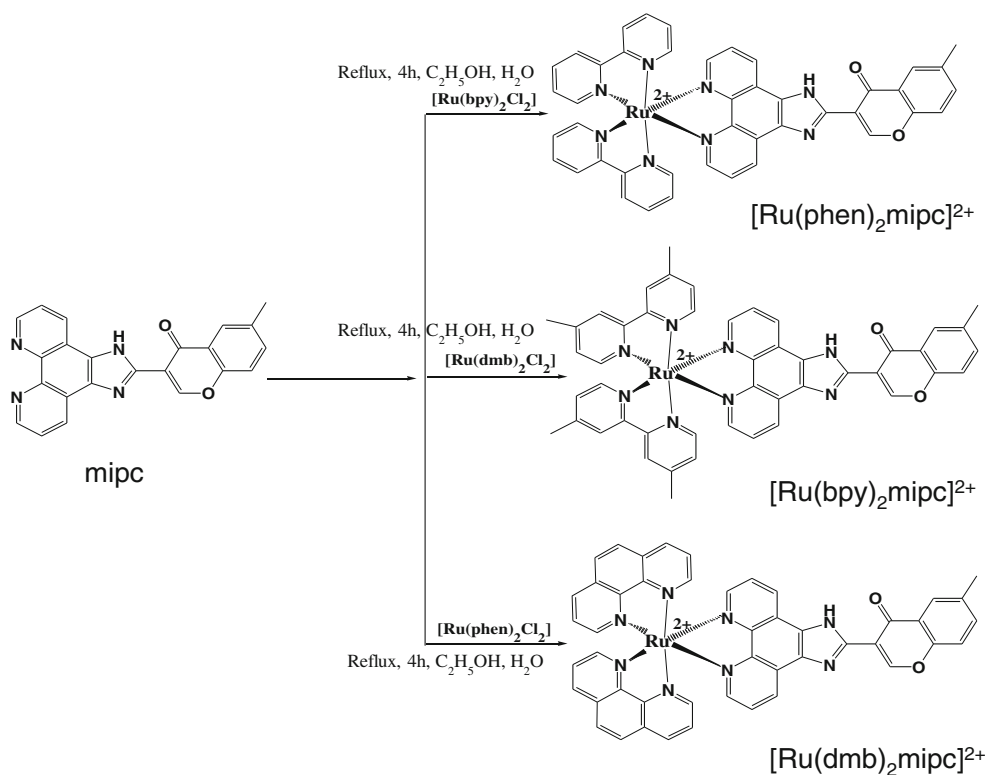
Synthesis of [Ru(dmb)₂(mipc)](ClO₄)₂. 2H₂O

This complex was synthesized in a manner identical to that described for 1, with cis-[Ru(dmb)₂Cl₂].2H₂O (0.290 g, 0.5 mmol) in place of cis-[Ru(dmp)₂Cl₂].2H₂O. Yield: 0.346 g (65 %). Anal. Found: C, 53.94; H, 3.69; N, 10.68. Calcd for C₄₇H₃₄Cl₂N₈O₁₂Ru: C, 53.93; H, 3.66; N, 10.70 %. ES-MS [CH₃CN, m/z]: 947.0

Physical Measurements

General Methods Elico-Spectrophotometer (Model: BL 198) was used for recording UV-vis absorption studies to determine the Kb values. KBr disks on a Perkin-Elmer FT-IR-1605 spectrometer was used to record IR spectroscopic data. The 400 MHz Standard NMR using DMSO-d₆ as the solvent and TMS as an internal standard Bruker ZGradient single axis fitted high resolution NMR Probe were used to measure the ¹H and ¹³C NMR spectral data. Perkin-Elmer 240 elemental analyzer was used to Micro analysis (C, H and N). Elico-Model SL 174 spectrofluorometer was used to

Fig. 1 Synthetic scheme of $\text{Ru}(\text{phen})_2\text{mipc}]^{2+}$ (1), $[\text{Ru}(\text{bpy})_2\text{mipc}]^{2+}$ (2), $[\text{Ru}(\text{dmb})_2\text{mipc}]^{2+}$ (3) from mipc as a starting material



record spectral data to determine K_b values. Ostwald Viscometer was used for viscosity measurements.

DNA Binding Experiments The DNA binding experiments were performed in Tris–HCl buffer at 25 °C. The absorption titrations were performed at a fixed complex concentration, to which the DNA stock solution was gradually added up to the point of saturation. The mixture was allowed to equilibrate for 5 min before the spectra were recorded. The intrinsic binding constants, K_b , of the Ru (II) complexes bound to DNA were calculated from Eq. (1) [45].

$$[\text{DNA}] / (\varepsilon_a - \varepsilon_f) = [\text{DNA}] / (\varepsilon_b - \varepsilon_f) + 1 / K_b (\varepsilon_b - \varepsilon_f) \quad (1)$$

Where $[\text{DNA}]$ is the concentration of DNA, ε_a , ε_f and ε_b corresponds to the apparent absorption coefficient $A_{\text{obsd}}/[\text{complex}]$, the extinction coefficient for the free complex and the extinction coefficient for the complex in the fully bound form, respectively. In plots of $[\text{DNA}]/(\varepsilon_a - \varepsilon_f)$ versus $[\text{DNA}]$, K_b is given by the ratio of slope to the intercept.

The emission intensities were recorded in the range of 520–720 nm. In these emission studies fixed metal complex concentration (10 μM) was taken and to this varying concentration (0–100 μM) of DNA was added. The excitation wavelength was fixed and the emission range was adjusted before measurements. The fraction of the ligand bound was calculated from the relation $C_b = C_t [(F - F_0)/F_{\text{max}} - F_0]$,

Table 1 ^1H NMR data of $[\text{Ru}(\text{phen})_2\text{mipc}]^{2+}$ (1), $[\text{Ru}(\text{bpy})_2\text{mipc}]^{2+}$ (2), $[\text{Ru}(\text{dmb})_2\text{mipc}]^{2+}$ (3) and mipc and also these IR data

| Complex | IR data (cm^{-1}) $\nu_{\text{N-H}}$ $\nu_{\text{C=C}}$ $\nu_{\text{C=N}}$ $\nu_{\text{M-N}}$ | ^1H NMR data (40 MHz, ppm DMSO- d_6 , TMS) |
|----------------------------------------------|-------------------------------------------------------------------------------------------------------------|--------------------------------------------------------------------------------------------------------------------------------------------------------------------------------------------------------------|
| mipc (ligand) | 3400 1481 1643 – | δ 8.87 (s, 1H), 8.06 (s, 1H), 7.38 (t, 1H), 7.63 (s, 1H), 7.44 (s, 1H), 7.30 (d, 1H), 6.89 (d, 1H), 2.31 (s, 3H) |
| $[\text{Ru}(\text{phen})_2\text{mipc}]^{2+}$ | 3402 1427 1600 624 | δ 9.21 (s, 1H), 8.8 (d, 2H), 8.54 (d, 2H), 8.50 (d, 2H), 8.36 (s, 4H), 8.18 (d, 2H), 7.90 (d, 2H), 7.98 (m, 4H), 7.58 (d, 1H), 7.50–7.60 (m, 6H), 3.07 (s, 3H). |
| $[\text{Ru}(\text{bpy})_2\text{mipc}]^{2+}$ | 3406 1444 1616 624 | δ 9.11 (s, 1H), 8.84 (d, 2H), 8.62 (d, 2H), 8.60 (d, 2H), 8.00 (t, 2H), 7.87 (t, 3H), 7.75 (d, 2H), 7.69 (m, 3H), 7.65 (d, 2H), 7.51 (m, 2H), 7.42 (d, 1H), 7.37 (t, 2H), 7.11 (t, 2H), 3.02 (s, 3H). |
| $[\text{Ru}(\text{dmb})_2\text{mipc}]^{2+}$ | 3406 1444 1600 624 | δ 9.22 (d, 1H), 9.10 (s, 1H), 8.79 (d, 1H), 8.50 (d, 4H), 8.04 (s, 4H), 7.81 (d, 2H), 7.65 (d, 1H), 7.50–7.55 (m, 2H), 7.41 (d, 1H), 7.18 (d, 4H), 6.91 (d, 1H), 3.06 (s, 3H), 2.37 (s, 12H). |

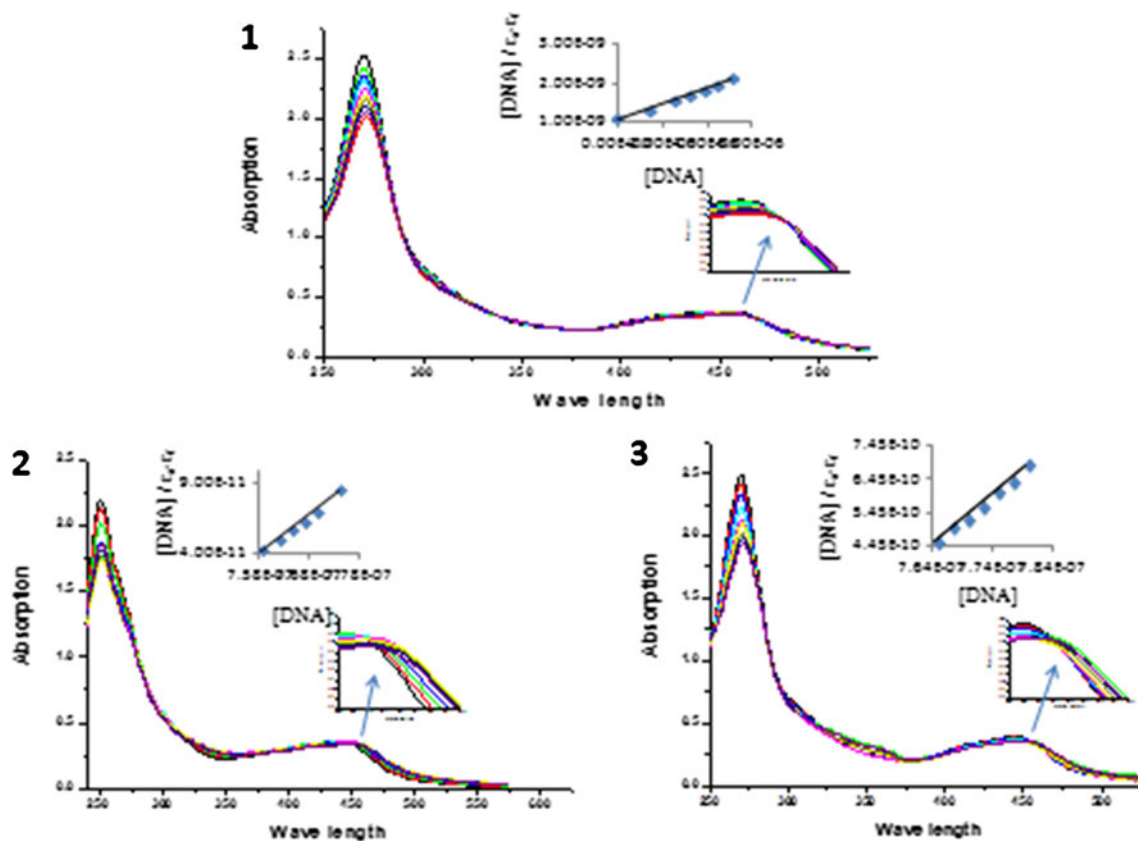


Fig. 2 Absorption spectra of $[\text{Ru}(\text{phen})_2\text{mipc}]^{2+}$ (1), $[\text{Ru}(\text{bpy})_2\text{mipc}]^{2+}$ (2), $[\text{Ru}(\text{dmb})_2\text{mipc}]^{2+}$ (3) with isosbestic point

where C_t is the total complex concentration, F is the observed fluorescence emission intensity at a given DNA concentration, F_0 is the intensity in the absence of DNA and F_{max} is when the complex is fully bound to DNA. Binding constant (K_b) was obtained from a modified Scatchard equation [46], From a Scatchard plot of r/C_f vs r , where r is the $C_b/[\text{DNA}]$ and C_f is the concentration of free complex.

Viscosity experiments were carried out on Ostwald viscometer, placed in thermo stated water-bath maintained at 30 ± 0.1 °C. CT-DNA samples approximately 200 bp in average length were prepared by sonication in order to minimize the complexes arising from DNA flexibility [47]. Data were presented as $(\eta/\eta^0)^{1/3}$ versus concentration of $[\text{Ru}(\text{II})]/[\text{DNA}]$, where η is viscosity of DNA in the presence of the complex and η^0 is the viscosity of DNA alone. Viscosity values were calculated from the observed flow time of DNA-containing solutions ($t > 100$ s) corrected for the flow time of the buffer alone (t_0) [48].

Super coiled pBR-322 DNA (50 μM) was used for the gel electrophoresis experiments, super coiled DNA was treated with Ru(II) complexes with 20–80 mM range in Tris–HCl, 18 mM NaCl buffer pH 7.8 and the solutions were then irradiated at room temperature with a UV lamp (365 nm, 10 W). The samples were analyzed by electrophoresis for 1 h at 60 V on a 1 % agarose gel in Tris–acetic acid–EDTA

buffer, pH 7.2. The gel was stained with $1 \mu\text{gml}^{-1}$ ethidium bromide and photographed under UV-light.

The antimicrobial tests were performed by the standard disk diffusion method. The complexes were screened for their antimicrobial activity against viz. E. coli and S. aureus. A concentration of 1 mg/ml and (1,000 μM) 0.5 mg/ml (500 μM) of each Ru(II) complex compound in DMSO solution was prepared for testing against spore germination of each fungus. Filter paper disks of 5 mm size were prepared using Whatman filter paper no.1 (sterilized in an autoclave) saturated with 10 μl of the Ru(II) complex compounds dissolved in DMSO solution or DMSO as negative control. The fungal culture plates were inoculated and incubated at 25 ± 0.2 °C for 48 h. The plates were then observed and the diameters of the inhibition zones (in mm) were measured and tabulated. The results were also compared with standard antimicrobial drug streptomycin at the same concentration.

Driven by ever-increasing computational resources molecular simulation methods have become increasingly important to understand (bio) molecular function in the last decades. The DNA sequenced (CCAACGTTGG) obtained from the Protein Data Bank (PDB: 2194) at resolution 1.5 \AA was used for docking studies. Receptor (DNA) and ligand (complex) files were prepared using Mol2 format, Mercury (version 2.2) and

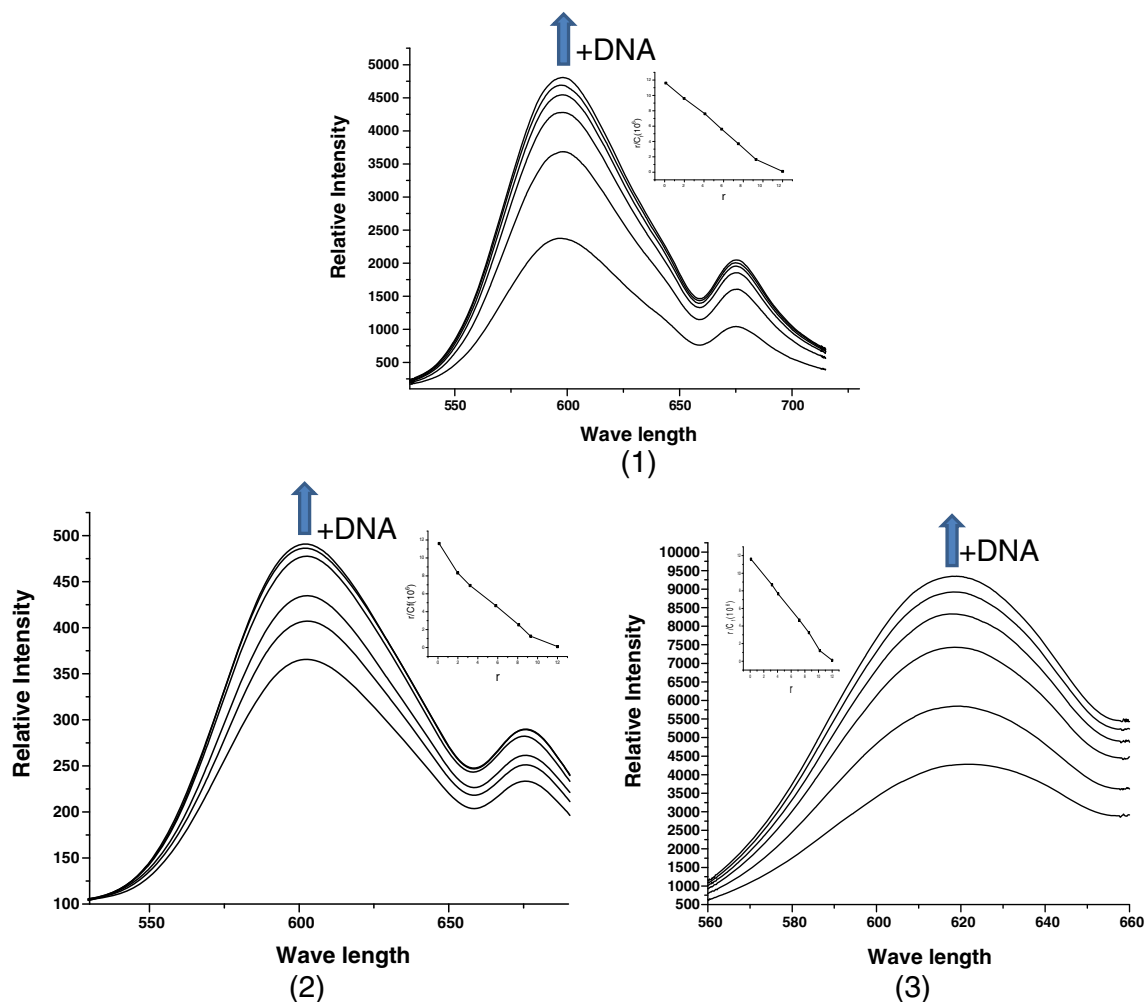


Fig. 3 Emission spectra of $[\text{Ru}(\text{phen})_2\text{mipc}]^{2+}$ (1), $[\text{Ru}(\text{bpy})_2\text{mipc}]^{2+}$ (2), $[\text{Ru}(\text{dmb})_2\text{mipc}]^{2+}$ (3) in clock wise direction, upward arrow in graphs indicates increase in intensity with DNA additions

GOLD DOCK 3.0.1 was employed for all docking calculations. All other parameters were default settings. For each of the docking cases, the lowest energy docked conformation, according to GOLD DOCK scoring function, was selected as the binding mode. The docking procedure depended on two principal features, (1) an energy (or scoring) function for evaluating trial configurations of the two interacting molecules and (2) an algorithm for seeking the best achievable minimum of this function. The two interacting molecules were considered as rigid bodies, and the sum of the van der Waals, hydrogen bonding and electrostatic energy terms were used as the scoring function.

Standard MTT assay procedures were used [49]. Cells were placed in 96-well micro assay culture plates (8×10^3 cells per well) and grown overnight at 37 °C in a 5 % CO_2 incubator. The complexes tested were dissolved in DMSO and diluted with RPMI 1640 and then added to the wells to achieve final concentrations ranging from 10^{-6} to 10^{-4} molL^{-1} . Control wells were prepared by addition of culture

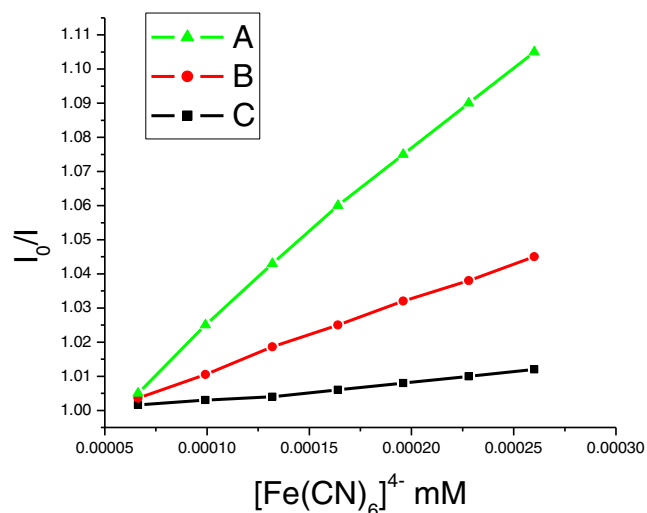


Fig. 4 Quenching of $[\text{Ru}(\text{phen})_2\text{mipc}]^{2+}$ (1), with $[\text{Fe}(\text{CN})_6]^{4-}$ quencher in absence (A) and presence of DNA (B and C)

Table 2 K_b values of absorption and emission spectral studies and K_{sv} values

| Name of the Complex | Abs K_b Values M^{-1} | Emission K_b Values M^{-1} | K_{sv} |
|--------------------------------------------|---------------------------|--------------------------------|----------|
| [Ru(phen) ₂ mipc] ⁺² | 5.32×10^4 | 7.58×10^4 | 158 |
| [Ru(bpy) ₂ mipc] ⁺² | 4.67×10^4 | 5.63×10^4 | 290 |
| [Ru(dmb) ₂ mipc] ⁺² | 3.63×10^4 | 4.71×10^4 | 501 |

medium (100 mL). Wells containing culture medium without cells were used as blanks. The plates were incubated at 37 °C in a 5 % CO₂ incubator for 48 h. Upon completion of the incubation, stock MTT dye solution (20 mL, 5 mgmL⁻¹) was added to each well. After 4 h incubation, buffer (100 mL) containing DMF (50 %) and sodium dodecyl sulfate (20 %) was added to solubilize the MTT. The optical density of each well was then measured on a micro plate spectrophotometer at a wavelength of 490 nm. The IC₅₀ values were determined by plotting the percentage of viability versus concentration on a logarithmic graph and reading of the concentration at which 50 % of cells remained viable relative to the control. Each experiment was repeated at least three times to obtain mean values. Tumor of **HeLa** cell lines were the subjected to this study.

Results and Discussion

Synthesis and Characterisation

The synthetic routs to mipc and its Ru(II) complexes 1, 2 and 3 are presented in Fig. 1. The ligand, mipc is synthesized by using a similar method to that described by Steck and Day [50]. condensation of 1,10- phenanthroline-5, 6-dione with the appropriate, mole ratio of 6-methyl-4-oxo-4H-chromene-3-carbaldehyde and ammonium acetate was refluxed in glacial

Fig. 5 Luminescence modulation routes of [Ru(phen)₂mipc]²⁺ in the absence and presence of DNA by Co²⁺ ion and EDTA, respectively

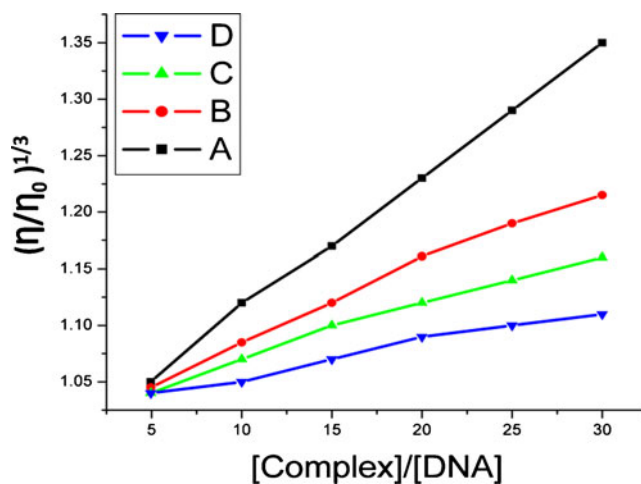
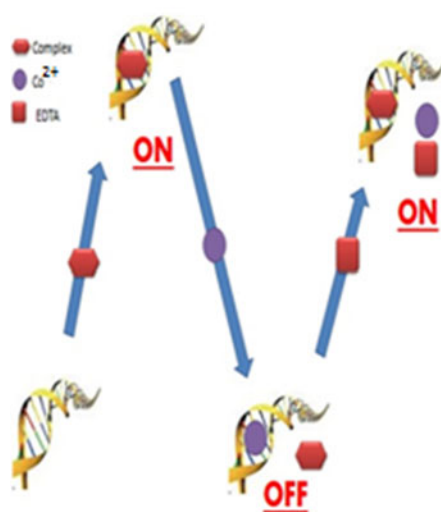


Fig. 6 Comparative viscosity studies of [Ru(phen)₂mipc]⁺²(1), [Ru(bpy)₂mipc]⁺²(2), [Ru(dmb)₂mipc]⁺²(3) with ct-DNA

acetic acid for 2 h. Complexes 1, 2 and 3 were prepared with appropriate mole ratios as explained above.

Three complexes and mipc were characterized by ¹H-NMR, IR spectra mass spectroscopy and elemental analysis. From IR stretching frequency region of M → L two peaks appeared at 721 cm⁻¹ for M → L of metal with ancillary ligand nitrogen and 624 cm⁻¹ for M → L of metal with mipc nitrogen it indicates that all six M → N bonds are not identical. The ¹H NMR and IR data were shown in Table 1.

Spectral Characteristics

Absorption Spectra

Electronic Spectroscopy is an important technique to be applied to DNA binding studies [15]. Complex binding with DNA via intercalation usually results in hypochromism and bathochromism, due to the intercalative mode involving a

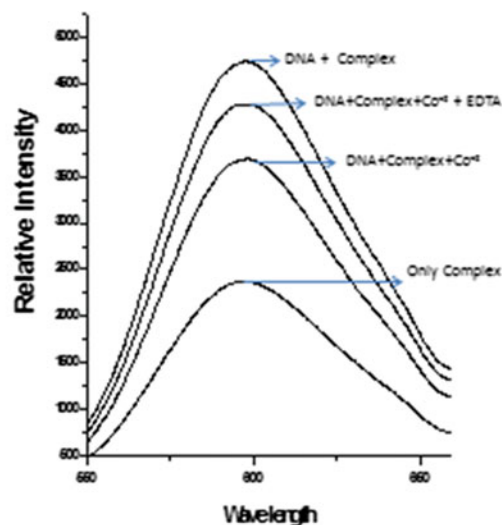


Table 3 Minimum inhibition concentration (MIC) of complexes ($\mu\text{g/ml}$): $[\text{Ru}(\text{phen})_2\text{mipc}]^{2+}$ (1), $[\text{Ru}(\text{bpy})_2\text{mipc}]^{2+}$ (2), $[\text{Ru}(\text{dmb})_2\text{mipc}]^{2+}$ (3)

| Complex | Bacterial Inhibition zone conc (1,000 μM) | | Bacterial Inhibition zone conc (500 μM) | |
|----------------------------------------------|-------------------------------------------------------|--------|-----------------------------------------------------|--------|
| | S.aureus | E.Coli | S.aureus | E.Coli |
| DMSO | – | – | – | – |
| $[\text{Ru}(\text{phen})_2\text{mipc}]^{2+}$ | 14 | 12 | 09 | 07 |
| $[\text{Ru}(\text{bpy})_2\text{mipc}]^{2+}$ | 12 | 10 | 08 | 05 |
| $[\text{Ru}(\text{dmb})_2\text{mipc}]^{2+}$ | 11 | 09 | 05 | 04 |

strong stacking interaction between the aromatic chromophore and the base pairs of DNA. The extent of the hypochromism and red shift is commonly related to the intercalative binding strength [51]. The absorption spectra of complexes 1, 2 and 3 shown in the Fig. 2 each consist of three well resolved bands around 290 nm, 360 nm and 470 nm respectively. The bands at 290 nm and 360 nm are attributed to intraligand $\pi \rightarrow \pi^*$ transitions [23]. The lowest energy band, around 470 nm is assigned to the metal-ligand charge transfer ($d_{\text{Ru}} \rightarrow \pi^*_{\text{mipc}}$). As the CT-DNA concentration is increased, the MLCT transition bands of complexes 1 at 472 nm, 2 at 473 nm and 3 at 474 nm exhibit hypochromism of 17, 12 and 7 % and bathochromism of 9, 6 and 4 nm, respectively along with isobestic points. Although these results are different from observations on the interaction of DNA with some reported mononuclear Ru(II) complexes [11, 52–54], which gave simultaneous decreases in absorption for both UV and visible (MLCT) bands, considering the spectral overlap with the MLCT transitions, these characteristics obviously suggest that the complex 1, 2 and 3 are most likely to interact with DNA through intercalation. Intrinsic binding constants, K_b of complexes 1, 2 and 3 are $5.32 \times 10^4 \text{M}^{-1}$, $4.67 \times 10^4 \text{M}^{-1}$, and $3.63 \times 10^4 \text{M}^{-1}$. Hence, binding is not as strong as that of their classical intercalators, such as $[\text{Ru}(\text{bpy})_2(\text{dppz})]^{2+}$ ($3.1 \times 10^6 \text{M}^{-1}$) [55] and $[\text{Ru}(\text{phen})_2(\text{dppz})]^{2+}$ ($5.1 \times 10^6 \text{M}^{-1}$) [23]. The difference between the binding constants of these complexes is due to different ancillary ligands. Complex 3 shows the less binding strength to double-helical DNA. Due to the presence of methyl groups on the 4 and 4' positions of the ancillary ligand, dmb causes steric hindrance when the complex intercalates into the DNA base pairs. Electron deficient rings interact more strongly with polyanion (DNA) than electron rich rings, so methyl group present on chromone ring may enhance the electron density on complex moiety and make electron denser, hence decreasing the binding constant and follows the order $1 > 2 > 3$.

Emission Spectral Studies

These three Ru(II) complexes in the absence of DNA can emit luminescence in Tris buffer with an emission maximum

appearing at 618–620 nm. Upon addition of CT DNA (Calf thymus DNA), emission intensities of complexes 1, 2 and 3 increased by a factor of 4.2, 3.5 and 3.4 times respectively shown in Fig. 3. This implies that complexes can strongly interact with DNA and protected by DNA efficiently, from the hydrophobic environment inside the DNA helix reduces the accessibility of solvent water molecules to the duplex and the complexes mobility is restricted at the binding site, which leads to decrease in the vibration modes of relaxation. The intrinsic binding constant from fluorescence data was obtained from a modified Scatchard equation [46], through a plot of r/C_f vs r where r is the $C_b/[\text{DNA}]$ and C_f is the concentration of the free metal complex. $C_b = C_t[(F - F_0)/F_{\text{max}} - F_0]$, where C_t is the total complex concentration, F is the observed fluorescence emission intensity at a given DNA concentration, F_0 is the intensity in the absence of DNA and F_{max} is the fully bound DNA to complex, binding constant is given by the slope. Scatchard plots for complexes have been constructed from luminescence spectra and binding constants (K_b) were $7.58 \times 10^4 \text{M}^{-1}$, $5.63 \times 10^4 \text{M}^{-1}$, and $4.71 \times 10^4 \text{M}^{-1}$. The binding constants obtained from luminescence titration with McGhee–von Hippel method is different from those obtained from absorption with the method suggested by Wolf et al. [45]. This difference between the two sets of binding constants should be caused by the different spectroscopy and different calculation method.

Quenching Studies

This observation was further supported by the emission quenching experiments using $[\text{Fe}(\text{CN})_6]^{4-}$ as quencher.

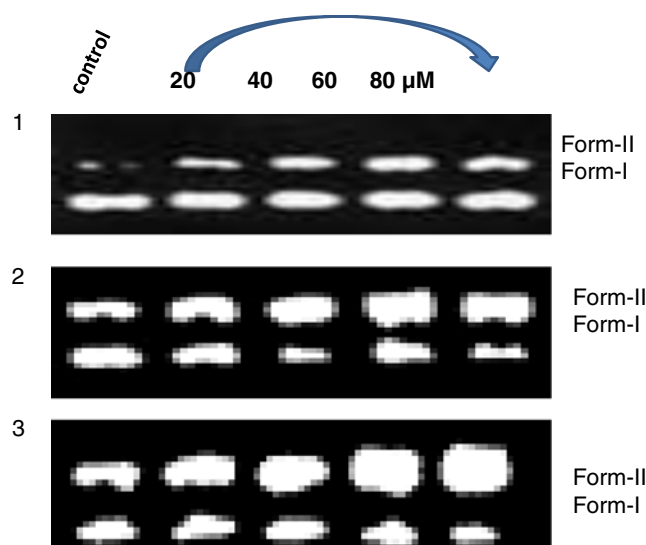


Fig. 7 Photoactivated cleavage studies of $[\text{Ru}(\text{phen})_2\text{mipc}]^{2+}$ (1), $[\text{Ru}(\text{bpy})_2\text{mipc}]^{2+}$ (2), $[\text{Ru}(\text{dmb})_2\text{mipc}]^{2+}$ (3) with 20 to 80 μM concentration ranges

Table 4 This table gives information about mode and no. of H-bonding and van der Waals forces with gold score

| Complex | H –Bond Donor-Acceptor | Bond Length (Å) | Vander Waals interactions (Complex – DNA) | Bond Length (Å) | Gold Score Fitness: |
|--------------------------------------------|------------------------|-----------------|-------------------------------------------|-----------------|---------------------|
| (a) | | | | | |
| [Ru(phen) ₂ mipc] ²⁺ | H68-DT8:O4 | 2.189 | C45-DC2:OP1 | 2.449 | 55.32 |
| | O34-DC1:H42 | 2.082 | C50- DC2:OP1 | 2.404 | |
| | O34-DC1:H42 | 2.024 | C44-DA3:OP1 | 2.602 | |
| | N21-DC2:H41 | 1.801 | H64-DA4:H62 | 1879 | |
| | | | C12-DA4: N6 | 2.697 | |
| | | | C36-DG9:OP1 | 2.629 | |
| | | | C26-DG10:O6 | 2.064 | |
| | | | H69-DC2:N4 | 2.713 | |
| | | | C20-DC1:H5 | 1.318 | |
| | | | H63-DA4:H62 | 1.888 | |
| (b) | | | | | |
| [Ru(bpy) ₂ mipc] ²⁺ | H77-DT7:O4 | 2.710 | C20-DC5:OP1 | 2.580 | 55.079 |
| | O52-DC1:H42 | 2.717 | C1- DA3:OP1 | 2.636 | |
| | O52-DC2:H42 | 2.220 | O52-DG10:O6 | 2.346 | |
| | N39-DC2:H41 | 2.100 | O52-DG9:O6 | 2.090 | |
| | | | C42-DG6:O6 | 2.626 | |
| (c) | | | | | |
| [Ru(dmb) ₂ mipc] ²⁺ | H68-DC1:N4 | 2.527 | H69-DT8:H71 | 1.433 | 54.8196 |
| | H68-DC2:N4 | 2.266 | H67-DT7:O4 | 1.853 | |
| | O34-DC1:H42 | 2.567 | H68-DC2:H41 | 1.822 | |
| | O34-DC1:H41 | 2.638 | H63-DC2:H41 | 1.721 | |
| | | | C33-DG10:N7 | 1.702 | |
| | | | C32-DG10:N7 | 2.533 | |
| | | | C2-DC5:OP1 | 2.475 | |
| | | | C3- DC5:OP1 | 2.723 | |
| | | | C41- DC2:OP1 | 2.322 | |
| | | | C3- DA4:N7 | 2.357 | |

Emission quenching with [Fe(CN)₆]⁴⁻ in the presence of DNA are shown in Fig. 4 for [Ru(Phen)₂MIPC]²⁺ complex. The complex binding to DNA can be protected from the quencher, because highly negatively charged [Fe(CN)₆]⁴⁻ would be repelled by the negative DNA phosphate backbone, hindering quenching of the emission of the bound complex. As illustrated in the presence of DNA complexes were efficiently quenched by [Fe(CN)₆]⁴⁻ resulting in linear Stern-Volmer plots. The Stern-Volmer quenching constant K_{sv} can be determined by using Stern-Volmer equation [47].

$$I_0 / I = 1 + K_{sv}[Q]$$

Where I_0 and I are the fluorescence intensities in the absence and presence of a quencher respectively, Q is the concentration of the quencher, K_{sv} is a linear Stern-Volmer quenching constant. Figure 4 shows the Stern-Volmer plots for the free complex in solution has high

K_{sv} than in the presence of DNA. Highly negatively charged quencher is expected to be repelled by the negatively charged phosphate backbone, and therefore a DNA bound cationic complex should be less quenched by anionic quencher, than the unbound complex [56, 57]. All the complexes show linear Stern-Volmer plots. The K_b and K_{sv} values have been given in Table 2.

It is therefore interesting to investigate that the photoluminescence of DNA-bound [Ru(phen)₂mipc]²⁺ could be tuned by successive introduction of Co²⁺ ions and EDTA. Figure 5 shows the decrease in the luminescence intensity of DNA-bound [Ru(phen)₂mipc]²⁺ due to the interactions of Co²⁺ with DNA. While further adding EDTA into the buffer system containing DNA-bound [Ru(phen)₂mipc]²⁺ with Co²⁺ ion, the emission intensity is recovered based on the strong coordination of Co²⁺ to EDTA. The luminescent change of DNA-bound [Ru(phen)₂mipc]²⁺ in the presence of Co²⁺ and EDTA reveals the modulation of Co²⁺ and

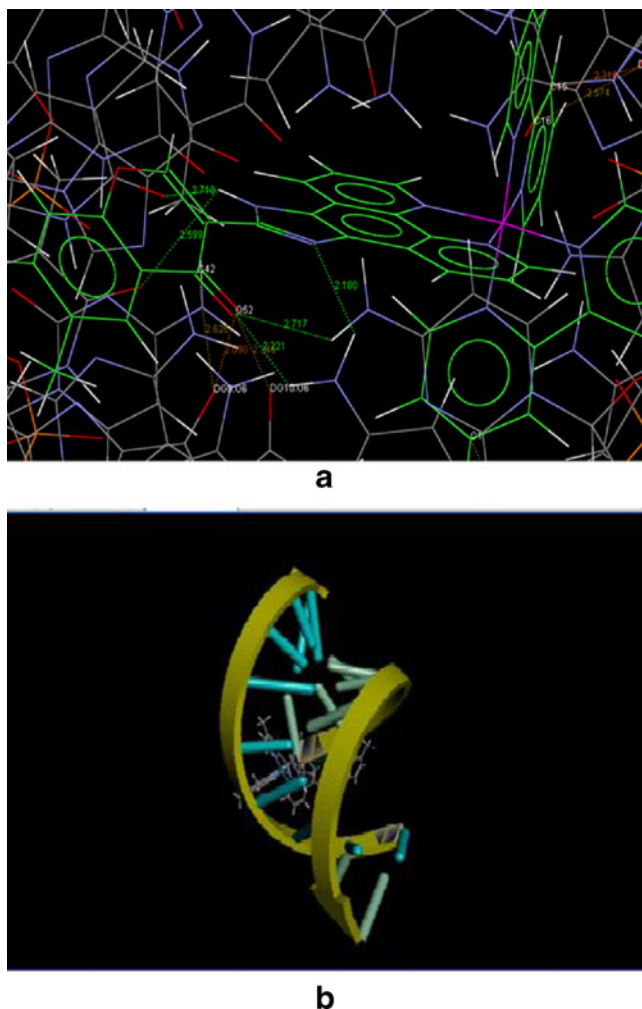


Fig. 8 Docking mode binding of Ru(II) polypyridyl complexes with PDB DNA, in fig(a) it is giving about H-bonding and fig(b) is showing interaction mode of complex into the DNA base pairs

EDTA to luminescence intensities of DNA-bound [Ru(phen)₂mipc]²⁺ (Fig. 5).

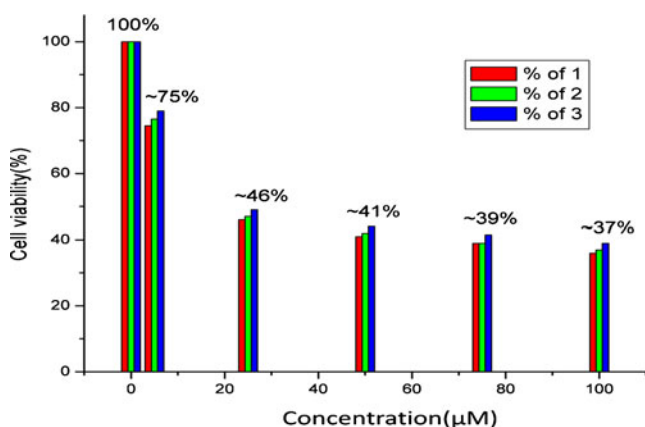


Fig. 9 Cell viability of HeLa cell lines in vitro treatment with complexes 1, 2 and 3. Each data point is the mean±standard error obtained from at least three independent experiments

Table 5 IC₅₀ values of [Ru(phen)₂mipc]⁺²(1), [Ru(bpy)₂mipc]⁺²(2), [Ru(dmb)₂mipc]⁺²(3) with HeLa cell lines

| Name of the Complex | IC ₅₀ Vales with respect to HeLa Cell lines |
|--------------------------------------------|--------------------------------------------------------|
| [Ru(phen) ₂ mipc] ⁺² | 21.87 % |
| [Ru(bpy) ₂ mipc] ⁺² | 23.31 % |
| [Ru(dmb) ₂ mipc] ⁺² | 24.27 % |

Viscosity Measurement

In general, nonclassical intercalation of a ligand can bend (or kink) the DNA helix, reducing its effective length and, concomitantly its viscosity, whereas classical intercalation of a ligand into DNA causes an increase in the viscosity of a DNA solution due to increased separation of the base pairs at the intercalation site and hence, an increase in the overall DNA molecular length [11, 45, 54, 58, 59]. On increasing the concentrations of Ru(II) complexes 1,2 and 3 the relative viscosities of CT-DNA decrease steadily. The decreased degree of viscosity, which may depend on the DNA-binding mode and affinity, follows the order of 1>2 >3 as shown in Fig. 6. Here intercalating ligand is same in all complexes, there is small difference in the viscosity, and this is due to the difference in the ancillary ligands. These further suggest that three Ru(II) complexes show an intercalative binding mode to CT-DNA, which parallel the absorption titration results.

Antimicrobial Studies

The antibacterial activity data (Table 3) indicate that the complexes showed considerable activity against *Staphylococcus aureus* and *Escherichia coli* at 1 mg/ml and 0.5 mg/ml concentrations. DMSO control showed a negligible activity as compared with the metal complexes. The experimental results of the compounds were compared against DMSO as the control and are expressed as inhibition zone diameter (in mm) vs control. The complexes were more effective against *Staphylococcus aureus* than *Escherichia coli*. [Ru(phen)₂mipc]²⁺ showed the highest activity 14 mm, 09 mm against *Staphylococcus aureus* at the concentrations of 1 mgml⁻¹ and 0.5 mg/ml. The same complex also showed an activity of 12 mm, 07 mm inhibition against *Escherichia coli*. The [Ru(bpy)₂mipc]²⁺ and [Ru(dmb)₂mipc]²⁺ complexes showed less activity against these bacteria than the first complex. It is evident from our results that all three metal complexes possess antibacterial activity. Earlier studies also showed results similar to those in this study [60].

Photo Activated Photocleavage Studies

Photo activated cleavage of pBR322 DNA. The cleavage reactions of plasmid DNA induced by these ruthenium (II)

complexes were monitored by agarose gel electrophoresis. Figure 7 shows gel electrophoresis separation of pBR322 DNA after incubation with two different concentrations of the complexes and irradiation at 365 nm for 30 min. No obvious DNA cleavage was observed for control experiments in which the complex was absent, or the plasmid was incubated with the complex in the dark. At increasing concentrations with 20 μM to 80 μM of complexes 1, 2 and 3 the amount of Form I (super coiled form) of pBR322 DNA diminished gradually, whereas that of Form II (circular form) increased. These results indicate that scission occurs on one strand (nicked). Under the same experimental conditions, complex 1 exhibits more effective DNA cleavage activity than complex 2 and 3, consistent with the DNA binding affinities of the complexes.

Molecular Docking of the Complex with DNA Sequence

A novel and robust automated docking method GOLD (Genetic Optimization for Ligand Docking) was used to predict the bound conformations of flexible ruthenium-complex (ligand) to B DNA (receptor) targets has been developed and tested, in combination with a new scoring function that estimates the free energy change upon binding. Molecular docking study was performed to understand the preferred orientation of sterically acceptable complex using 'Ru-mipc' with the DNA sequence. According to this docking experiment, complex reasonably binds with DNA sequence (CCAACGTTGG). Hypothetical structures resulting from the initial docking were energy-minimized. The minimum energy docked structure obtained suggested the best possible conformation of the ligand interaction mainly through carbonyl part of intercalating ligand to the DNA major groove. It has been observed that the Ru-complex is stabilized by electrostatic hydrogen bonding with DNA bases, particularly involving N7 of adenine, N3 of guanine, N1 of cytosine and thymine and Phosphate oxygen. Also considerable van der Waal's attractions (π - π) between Ru-complex and DNA chain.

Experimental results have shown that complexes 1, 2 and 3 can bind to DNA through interactive mode and complex one is with strong binding ability than other two. Our calculated results showed that the intercalative Ru-complex with four strong hydrogen bonds. From Table 4 and Fig. 8, it is clear that complex 1 binds through imidazo ring N, H (H68-DT8:O4), (N21-DC2:H41) and carbonyl Oxygen to Phosphate oxygen and NH_2 – Cytocine base pair (O34-DC1:H42), (O34-DC1:H42) through Hydrogen bonding with average bond length 2.042 \AA . In addition to H-bonds about ten van der Waal's attractions' between complex and DNA base pairs which enhancing binding ability. Similarly second and third Ru-complexes bind to DNA with four hydrogen bonds and van der Waal's forces of attraction

with average bond lengths 2.44 \AA ⁰ and 2.50 \AA ⁰ respectively. One more supporting evidence for the above order is gold scores fitness with complex-1 (55.32)>complex-2 (55.079)>complex-3 (54.8196) respectively. The order of H-bonding and gold fitness of molecular docking studies was exactly matching with spectroscopic results.

Cytotoxicity Assay in Vitro

The cytotoxicities of the three Ru(II) complexes in vitro assessed using the method of MTT reduction. Cisplatin was used as a positive control. After treatment of Hela cell lines for 48 h with complexes 1, 2 and 3 in a range of concentrations (5 μM –100 μM), the percentage inhibition of growth of the cancer cell was determined. The cell viabilities (%), obtained with continuous exposure for 48 h, are depicted in Fig. 9. The cytotoxicities of the complexes were found to be concentration dependent. The cell viability decreased with increasing concentrations of three complexes. The IC_{50} values were calculated in Table 5. Comparing IC_{50} values of 1, 2 and 3, 3 appeared to be more active than 1 and 2 against Hela cell lines. The cytotoxicities of these complexes are consistent with their DNA-binding activities. Furthermore, these complexes are lower in cytotoxicity than cisplatin under identical conditions.

Conclusions

Three ruthenium(II) complexes, $[\text{Ru}(\text{phen})_2\text{mipc}]^{2+}$ (1), $[\text{Ru}(\text{bpy})_2\text{mipc}]^{2+}$ (2) and $[\text{Ru}(\text{dmb})_2\text{mipc}]^{2+}$ (3) were synthesized and characterized. Absorption, emission, light switch effect studies and viscosity measurements suggest that 1, 2 and 3 interact with CT-DNA by intercalation. These complexes can bring about cleavage of plasmid DNA when irradiated at 365 nm and showing good antimicrobial activity against Ecoli and *Staphylococcus aureus*. The results from cytotoxicity assay show that 3 exhibits higher cytotoxic activity than 2 and 1 against selected tumor cell lines.

Acknowledgments We are grateful to DST PURSE project F.No A-30 for financial support and also CFRD & DBT- OU ISLARE Osmania University Hyderabad for helping the analysis and cytotoxic studies.

References

- Lippard SJ (1987) Chemistry and molecular biology of platinum anticancer drugs. *Pure Appl Chem* 59:731–742
- Salim A, Abu-Surrah MK (2006) Platinum Group Antitumor Chemistry: design and development of New Anticancer Drugs Complementary to Cisplatin. *Curr Med Chem* 13:1337–1357

3. Zhang Z, Bi C, Schmitt SM, Fan Y, Dong L, Jian Zuo Q, Dou P (2012) 1, 10-Phenanthroline promotes copper complexes into tumor cells and induces apoptosis by inhibiting the proteasome activity. *J Biol Inorg Chem* 17(8):1257–1267
4. Giovagnini L, Ronconi L, Aldinucci D, Lorenzon D, Sitran S, Fregona D (2005) Synthesis, Characterization, and Comparative in Vitro Cytotoxicity Studies of Platinum(II), Palladium(II), and Gold(III) Methyl sarcosine dithiocarbamate Complexes. *J Med Chem* 48:1588–1595
5. Perez-Rebolledo A, DaniloAyala J, de Lima GM, Marchini N, Bombieri G, Zani CL, Souza-Fagundes EM, Beraldo H (2005) Structural studies and cytotoxic activity of N(4)-phenyl-2-benzoylpyridine thiosemicarbazone Sn(IV) complexes. *Eur J Med Chem* 40(5):467–472
6. Liu J, Zheng W, Shi S, Tan C, Chen J, Zheng K, Ji L (2008) Synthesis, antitumor activity and structure–activity relationships of a series of Ru(II) complexes. *J Inorg Biochem* 102:193
7. Liu Y-J, Liang Z-H, Li Z-Z, Yao J-H, Huang H-L (2011) Ruthenium(II) Polypyridyl Complexes: synthesis and Studies of DNA Binding, Photocleavage, Cytotoxicity, Apoptosis, Cellular Uptake, and Antioxidant Activity. *DNA Cell Biol* 30(10):829–838
8. Li X, Xie Y-Y, Zhong N-J, Liang Z-H, He J, Huang H-L, Liu Y-J (2012) DNA-binding and photocleavage, cytotoxicity, apoptosis and antioxidant activity studies of ruthenium(II) complexes. *Transit Met Chem* 37:197–205
9. Puckett CA, Barton JK (2008) Mechanism of cellular uptake of a ruthenium polypyridyl complex. *Biochem* 47:11711–11716
10. Sigel A, Sigel H Eds. (1996) Metal ions in biological systems, interaction of metal ions with nucleotides, nucleic acids, and their constituents. Marcel Dekker, New York 32– 854
11. Pyle AM, Morii T, Barton JK (1990) Probing Microstructures in Double Helical DNA with Chiral Metal Complexes: recognition of Changes in Base-Pairs Propeller Twisting in Solution. *J Am Chem Soc* 112:9432
12. Sigman DS, Mazumdre A, Perrin DM (1993) Chemical nucleases. *Chem Rev* 93:2295–2316
13. Erkkila KE, Odom DT, Barton JK (1999) Recognition and Reaction of Metallointercalators with DNA. *Chem Rev* 99:2777
14. Ji LN, Zou XH, Liu JG (2001) Shape- and enantioselective interaction of Ru(II)/Co(III) polypyridyl complexes with DNA. *Coord Chem Rev* 513:216–217
15. Xiong Y, Ji LN (1999) Synthesis, DNA-binding and DNA-mediated luminescence quenching of Ru(II) polypyridine complexes. *Coord Chem Rev* 711:185–186
16. Pelligrini PP, Aldrich-Wright JR (2003) Evidence for chiral discrimination of ruthenium (II) polypyridyl complexes by DNA. *Dalton Trans* 3:176
17. Lawrence D, Vaidyanathan VG, Nair BU (2006) Synthesis, characterization and DNA binding studies of two mixed ligand complexes of ruthenium (II). *J Inorg Biochem* 100:1244
18. Maheswari PU, Palaniandavar M (2004) DNA binding and cleavage activity of [Ru(NH₃)₄(diimine)]Cl₂ Complexes. *Inorg Chim Acta* 357:901
19. Yang XJ, Drepper F, WU B, Sun WH, Haehnel W, Janiak C (2005) From model compounds to protein binding: synthesis, characterizations and fluorescence studies of [Ru^{II}(bipy)(terpy)L]²⁺ complexes (bipy = 2,2′ - bipyridine; terpy = 2,2′ : 6′,2″ - terpyridine; L = imidazole, pyrazole and derivatives, cytochrome c). *Dalton Trans* 21(2):256–267
20. Sava G, Pacer S, Berganmo A, Cocchetti M, Mestroni G, Allesio E (1995) Effects of ruthenium complexes on experimental tumors: irrelevance of cytotoxicity for metastasis inhibition. *Chem Biol Interact* 95:109–126
21. Beckford FA, Shalowski M Jr, Leblanc G, Thessbng J, Lesley C (2009) Microwave synthesis of mixed ligand diimine–thiosemicarbazone complexes of ruthenium (II): biophysical reactivity and Cytotoxicity. *Dalton Trans* 48:10757–10764
22. Morris RE, Aird RE, Murdoch PD, Chen HM, Cummings J, Hughes ND, Parsons S, Parkin A, Boyd G, Jodrell DI, Sadler PJ (2001) Inhibition of Cancer Cell Growth by Ruthenium(II) Arene Complexes. *J Med Chem* 44:3616–3621
23. Friedman AE, Chambron JC, Sauvage JP, Turro NJ, Barton JK (1990) Molecular “Light Switch” for DNA Ru(bpy)₂(dppz)²⁺. *J Am Chem Soc* 112:4960
24. Hartshorn RM, Barton JK (1992) Novel Dipyridophenazine Complexes of Ruthenium (II): exploring Luminescent Reporters of DNA. *J Am Chem Soc* 114:5919
25. Praveen Kumar Yata M, Shilpa P, Nagababu MR, Reddy LR, Kotha NM, Gabra SS (2012) Study of DNA Light Switch Ru(II) Complexes: synthesis, Characterization, Photocleavage and Antimicrobial Activity. *J Fluoresc* 22:835–847
26. Shobha Devi C, Yata Praveen Kumar P, Nagababu MS, Reddy R, Gabra NM, Satyanarayana S (2012) DNA binding characteristics of Ru(II) Complexes and their “light switch” on off effect in presence of Co(II) and EDTA. *J Iran Chem Soc* 9:671–680
27. Shobha Devi C, Satyanarayana S (2012) Synthesis, characterization and DNA - binding properties of Ru(II) molecular “light switch” complexes. *J Coord Chem* 65:474–486
28. Shilpa M, Penubaka Nagababu J, Naveen Lavanya Latha A, Gaytri Devi A, Nagarjuna YP, Kumar SS (2011) DNA-interactions of ruthenium(II) & Cobalt(III) phenanthroline and bipyridyl complexes with a planar aromatic ligand 2-(2 fluoronyl) 1H-imidazo [4,5-f][1,10-Phenanthroline]. *J Incl Phenom Macrocycl Chem* 70:187–195
29. Ashwini Kumar K, Reddy KL, Satyanarayana S (2010) Study of the interaction between ruthenium (II) complexes and CT-DNA, Synthesis, Characterization, Photocleavage and Antimicrobial activity studies. *Supramol Chem* 22:629–643
30. Vidhisha S, Reddy KL, Ashwini Kumar K, Satyanarayana S (2010) Synthesis, DNA interactions of ruthenium (II) complexes with polypyridyl ligand: 2-(2, 5-dimethoxyphenyl)-1H-imidazo [4, 5-f][1, 10]-phenanthroline. *Transit Met Chem* 35: 1027–1034
31. Ashwini Kumar K, Reddy KL, Satyanarayana S (2010) Synthesis, DNA interaction and Photocleavage studies of ruthenium(II) complexes with 2- (pyrrole) imidazo [4,5-f] [1,10-phenanthroline as an intercalative ligand. *Transit Met Chem* 35:713–720
32. Reddy KL, Harish Y, Reddy K, Satyanarayana S (2009) DNA-binding and Photocleavage properties of Ru(II) polypyridyl complexes with DNA and their toxicity studies on eukaryotic microorganisms. *Nucleosides Nucleotides Nucleic Acids* 28: 953–968
33. Ashwini Kumar K, Reddy KL, Satyanarayana S (2010) Synthesis, characterization and DNA binding studies of ruthenium(II) complexes with 2-benzo[b] furan-2-yl-1H-imidazo [4,5-f] [1,10] phenanthroline as an intercalative ligand. *J Coord Chem* 63:3676–3687
34. Nagababu P, Shilpa M, Ira Bhatnagar PBN, Sreenivas Y, Kumar P, Reddy KL, Satyanarayana S (2010) Synthesis, Characterization, DNA Binding Properties, Fluorescence Studies and Toxic activity of cobalt(III) and ruthenium(II) polypyridyl complexes. *J Fluoresc* 21(2):563–572
35. Shilpa M, Nagababu P, Kumar YP, Naveena J, Latha L, Rajender Reddy M, Satyanarayana S (2011) DNA-interactions of ruthenium(II) complexes with planar aromatic ligands. *J Fluoresc* 21:1155–1164
36. Liu XW, Li J, Li H, Zheng KC, Chao H, Ji LN (2005) Synthesis, characterization, DNA-binding and photocleavage of complexes Ru(phen)₂ (6-OH-dppz)²⁺ and [Ru(phen)₂ (6-NO₂ -dppz)]²⁺. *J Inorg Biochem* 99:2372–2380

37. Liu YJ, Wei XY, Mei WJ, He LX (2007) Synthesis, characterization and DNA binding studies of ruthenium (II) complexes: $[\text{Ru}(\text{bpy})_2(\text{dtmi})]^{2+}$ and $[\text{Ru}(\text{bpy})_2(\text{dtmi})]^{2+}$. *Trans Met Chem* 32:762–768
38. Tan LF, Chao H (2007) DNA-binding and photocleavage studies of mixed polypyridyl ruthenium (II) complexes with calf thymus DNA. *Inorg Chim Acta* 360:2016–2022
39. Liu JG, Ye BH, Li H, Zhen QX, Ji LN (1999) Polypyridyl ruthenium(II) complexes containing intramolecular hydrogen-bond ligand: syntheses, characterization and DNA-binding properties. *J Inorg Biochem* 76:265–271
40. Perrin D, Annarego WLF, Perrin DR (1980) Purification of laboratory chemicals, 2nd edn. Pergamon Press, New York
41. Marmur J (1961) A procedure for the isolation of deoxyribonucleic acid from micro-organisms. *J Mol Biol* 3:208–218
42. Reichmann ME, Rice SA, Thomas CA, Doty P (1954) Crystalline Δ^4 -Androsten-17 β -o1-3, 16-dione. *J Am Chem Soc* 76:3047–3053
43. Yamada M, Tanaka Y, Yoshimoto Y, Kuroda Shimao S (1992) Synthesis and properties of diamino-substituted dipyrido [3, 2-a: 20, 30-c] phenazine. *J Bull Chem Soc Jpn* 65:1006–1011
44. Sullivan BP, Salmon DJ, Meyer T (1978) Mixed Phosphine 2, 2'-Bipyridine Complexes of Ruthenium. *Inorg Chem* 17:3334–3341
45. Wolfe A, Shimer GH, Meehan T (1987) Polycyclic aromatic hydrocarbons physically intercalate into duplex regions of denatured DNA. *Biochemistry* 26:6392–6396
46. Mc Ghee JD, Von Hippel PH (1974) Theoretical aspects of DNA-protein interactions: co-operative and non-co-operative binding of large ligands to a one-dimensional homogeneous lattice. *J Mol Biol* 86:469–489
47. Chaires JB, Dattagupta N, Crothers DM (1982) Self association of daunomycin. *Biochemistry* 21:3927–3932
48. Satyanarayana S, Dabrowiak JC, Chaires JB (1993) Tris (phenanthroline) ruthenium (II) enantiomer interactions with DNA: mode and specificity of binding. *Biochemistry* 32:2573–2584
49. Tselepi-Kalouli E, Katsaros N (1989) The Interaction of $[\text{Ru}(\text{NH}_3)_5\text{Cl}]^{2+}$ and $[\text{Ru}(\text{NH}_3)_6]^{3+}$ ions with DNA. *J Inorg Biochem* 37:271–282
50. Steck EA, Day AR (1943) Reactions of Phenanthraquinone and Retenequinone with Aldehydes and Ammonium Acetate in Acetic Acid Solution. *J Am Chem Soc* 65:452
51. Tan L, Shen J, Liu J, Jin LZL, Weng C (2012) Spectral characteristics, DNA-binding and cytotoxicity of two functional Ru(II) mixed-ligand complexes. *Dalton Trans* 41:4575
52. Zhou XH, Ye BH, Li H, Liu JG, Xiang Y, Ji LN (1999) Mono and bi-nuclear ruthenium(II) containing a new asymmetric ligand 3-(pyrazin-2-yl)-as-triazino[5,6-f]1,10-phenanthroline: synthesis, Characterization and DNA-binding properties. *J Chem Soc Dalton Trans* 9:1423
53. Nair RB, Teng ES, Kirkland SL, Murphy CJ (1998) Synthesis and DNA-binding properties of $[\text{Ru}(\text{NH}_3)_4\text{dppz}]^{2+}$. *Inorg Chem* 37:139–141
54. Moucheron C, Mesmaeker AKD, Choua C (1997) Photophysics of $\text{Ru}(\text{phen})_2(\text{PHEHAT})^{2+}$: a Novel “Light Switch” for DNA and Photo-oxidant for Mononucleotides. *Inorg Chem* 36:584–592
55. Gao F, Chao H, Zhou F, Yuan YX, Peng B, Ji LN (2006) DNA interactions of a functionalized ruthenium(II) mixed-polypyridyl complex $[\text{Ru}(\text{bpy})_2\text{ppd}]^{2+}$. *Inorg Biochem* 100:1487–1494
56. Joseph R, Lakowicz GW (1973) Quenching of fluorescence by oxygen. Probe for structural fluctuations in macromolecules. *Biochemistry* 12:4161–4170
57. Lakowicz JR (1983) Principles of fluorescence spectroscopy. Plenum Press, New York
58. Drew WL, Barry AL, Toole RO, Sherris JC (1972) Clinical Microbiology and Immunology Reliability of the Kirby-Bauer Disc Diffusion Method for Detecting Methicillin-Resistant Strains of *Staphylococcus aureus*. *Appl Environ Microbiol* 24:240
59. Satyanarayana S, Dabrowiak JC, Chaires JB (1992) Neither delta-nor lambda- tris- (phenanthroline) ruthenium (II) binds to DNA by classical intercalation. *Biochemistry* 31:9319
60. Ashwini Kumar K, Kotha Laxma Reddy S, Vidhisha SS (2009) Synthesis, Characterization and DNA binding and Photocleavage studies of $[\text{Ru}(\text{bpy})_2\text{BDPPZ}]^{2+}$, $[\text{Ru}(\text{dmb})_2\text{BDPPZ}]^{2+}$ and $[\text{Ru}(\text{phen})_2\text{BDPPZ}]^{2+}$ complexes and their antimicrobial activity. *Appl Organomet Chem* 23:409–420